RESEARCH ARTICLE

Particle & Particle Systems Characterization
www.particle-journal.com

Synthesis of Anisotropic Gold Microparticles via L-Glutathione-Mediated Pathways in Droplet Microfluidics

*Zhenxu Yang, Qiankun Yin, Mengfan He, Shin-Wei Chong, Zhejun Xu, Xiaochen Liu, Christopher Vega-Sánchez, Arun Jaiswal, Daniele Vigolo, and Ken-Tye Yong**

Microfluidic-assisted synthesis of nanoparticles has generated significant interest for its precise control and high throughput capabilities. Among various nanomaterials, gold nanoparticles (AuNPs) have shown remarkable potential in numerous applications, such as disease detection, photothermotherapy, drug delivery, and even defense applications. Recent synthesis strategy of peptide-mediated method has sparked greater interest by offering unique chiroptical properties and their applications in biomedical applications. In this study, the use of droplet microfluidics is explored for the synthesis of peptide-mediated AuNPs, aiming to accelerate automated production via flow chemistry. This method leads to the formation of anisotropic gold particles, with sizes ranging from hundreds of nanometers to the micron scale. The interfacial energy is identified at the water/oil interface as a critical factor influencing this outcome, with L-glutathione (L-GSH) playing a significant role in the development of hyper-branched structures. These results demonstrate the capability of droplet microfluidics in producing anisotropic gold particles at micron scales, presenting new possibilities for the advancement of nanoparticle synthesis techniques.

1. Introduction

Microfluidic-assisted production of nanoparticles has gained attention in both academia and industry in recent years due to microfluidics' potential in good controllability of fluid flow and potential of high throughputs.[1–4] Inevitably, different types of nanomaterials have been translated into this production method, such as nano-liposomes,[5] carbon quantum dots,[6,7] and metal oxides.[8–10] In particular, due to promising applications demonstrated by gold nanoparticles (AuNPs) in disease detection,[11–13] photothermotherapy,[14,15] drug delivery,[16] and even defense applications,[17] the synthesis of gold nanoparticles using microfluidic devices has also been a keen focus.[18–22] Recently, the use of peptide in modulating seed-mediated growth of gold nanoparticles has sparked interest in peptide-mediated synthesis strategies,[23–25] showing interesting chiroptical responses and tissue engineering prospects.[26,27] In an attempt to translate bulk solution-based synthesis strategy of peptide-mediated gold nanoparticles, we adopted droplet microfluidic device for such purpose, hoping to accelerate the automated production of AuNPs via flow chemistry in the future.[28–30]

Amino acids and peptides have been demonstrated to produce AuNPs.[31–33] Although many reports have shown the ability to form sub-100 nm sized NPs,[32,34] only a handful reported biomolecules' capability in large particle formation beyond 1 μm range.[35–39] Recent awareness of sustainable synthesis of nanoparticles have also brough the focus into microfluidics,[40,41] that offers different designs to support the requirements of a diverse range of nanoparticle synthesis.[42–44] Interestingly, droplet microfluidics have been shown the ability

Z. Yang, Q. Yin, M. He, S.-W. Chong, Z. Xu, X. Liu, A. Jaiswal, D. Vigolo, K.-T. Yong
School of Biomedical Engineering
Faculty of Engineering
The University of Sydney
Sydney, New South Wales 2006, Australia
E-mail: ken.yong@sydney.edu.au

The ORCID identification number(s) for the author(s) of this article can be found under https://doi.org/10.1002/ppsc.202400056

DOI: 10.1002/ppsc.202400056

Z. Yang, Q. Yin, Z. Xu, X. Liu, A. Jaiswal, K.-T. Yong
The Biophotonics and Mechanobioengineering Laboratory
Faculty of Engineering
The University of Sydney
Sydney, New South Wales 2006, Australia

Z. Yang, Q. Yin, S.-W. Chong, Z. Xu, X. Liu, A. Jaiswal, D. Vigolo, K.-T. Yong
The University of Sydney Nano Institute
The University of Sydney
Sydney, New South Wales 2006, Australia

C. Vega-Sánchez
School of Electromechanical Engineering
Costa Rica Institute of Technology
Cartago 159-7050, Costa Rica

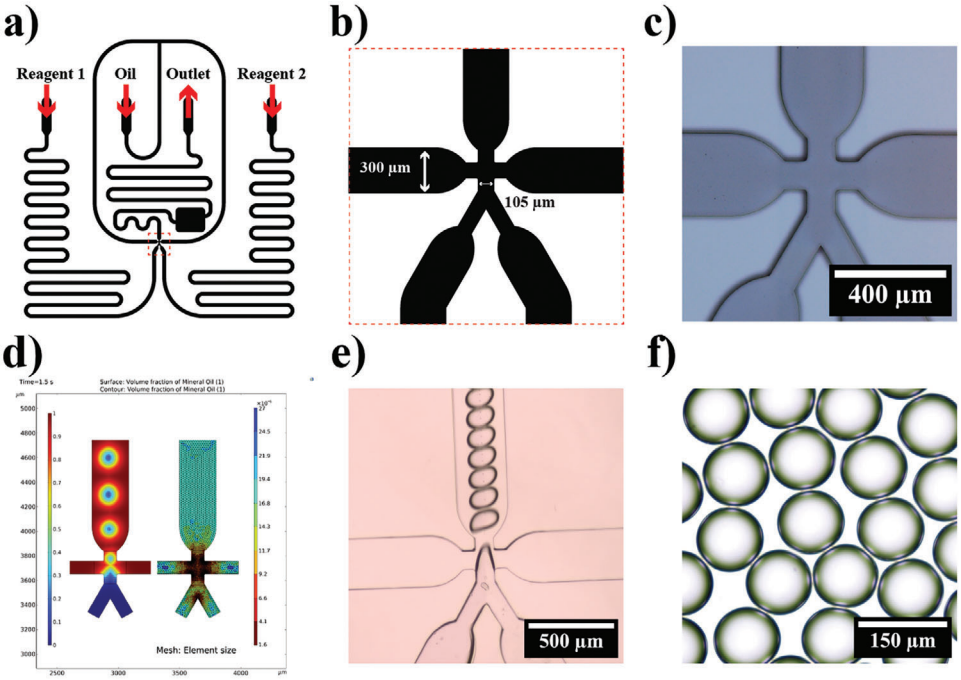

Figure 1. Design, simulation, and testing of the droplet microfluidics. a) Schematic sketch of the two reagents droplet microfluidic device with an incubation viewing port. b) An enlarged detailed one the droplet microfluidic device's cross section. c) An optical image of the master at the cross section. d) COMSOL simulation of the droplet production (left) and a visualization of the mesh size (physics-based fine mesh). e) An optical microscope image of droplet formation of the produced device. f) An optical microscope image of the droplets at the incubation viewing window.

to control the size of the gold particles.[45] However, previous reports have shown that emulsion assisted AuNPs could produce dendritic structures instead.[46] Specifically, it seems that the oil/water interface may play a role in modulating AuNPs formation.

In this study, we investigate the impact of oil/water interface on the formation of gold nanoparticles (AuNPs) using droplet microfluidics and explore methods of anisotropic particle synthesis. Since L-glutathione (L-GSH) has previously demonstrated its ability to direct anisotropic chiroptical AuNPs,[47] we choose this chemical for our synthesis condition. We herein report the production of anisotropic gold nanoparticles (AuNPs) with sizes ranging from a few hundred nanometers to the micron range using droplet microfluidics. The mechanisms behind the formation of these anisotropic AuNPs is yet to be fully understood. However, the system's simplicity enables the generation of various morphological shapes through minor changes in solution composition, including the production of hyper-branched structures at micron scales in a short timeframe. We attribute this formation to the role of the water/oil interface and the use of L-GSH.

2. Results and Discussion

2.1. Droplet Microfluidics

Different types of microfluidics have already been utilized to produce AuNPs. Some achieved high controllability over the morphology of the AuNPs in segmented flow,[48] while some were able to demonstrate the ability to continuously produce AuNPs without the need for introducing immiscible fluids.[49] Previous work by Shin et al. demonstrated the emulsion assisted production of branched particles under continuous stirring.[46] Drawing inspirations from it, we have translated the mechanically induced emulsion into chemically governed emulsion system via droplet microfluidic to create a stable emulsion system of simple surfactant-oil system. The droplet microfluidic device has the advantage of producing stable droplets at consistent sizes,[50] and has previously demonstrated the ability to produce large anisotropic gold particles.[51]

2.1.1. Simulation and Fabrication of Droplet Microfluidics

To gain full control of the microfluidic device parameters, we designed and fabricated a two-reagent droplet microfluidic device, a modified design adopted from Dolomite, Ltd., UK (µEncapsulator 2 Reagent Droplet Chip, 3200527).[52] A viewing window is designed to observe the droplet stability in-device and to serve as an incubation chamber by temporarily slowing down the droplets existing the device, as shown in **Figure 1a**. To induce mixing in the droplets, serpentine structures immediately follow the cross junction.[53] The fluid path in the main channel has a width of 300 µm where the orifice has a narrower width of 105 µm (Figure 1b). Prior to the fabrication of the master mold, we performed a COMSOL Multiphysics (6.1) computational fluidic dynamics (CFD) simulation to validate the cross-junction design. The simulation focused on the validation of the orifice design (105 µm), where a two-phase flow level-set simulation was conducted (Supporting Information). As demonstrated in Figure 1d, the 2D simulation showed a positive result of droplet

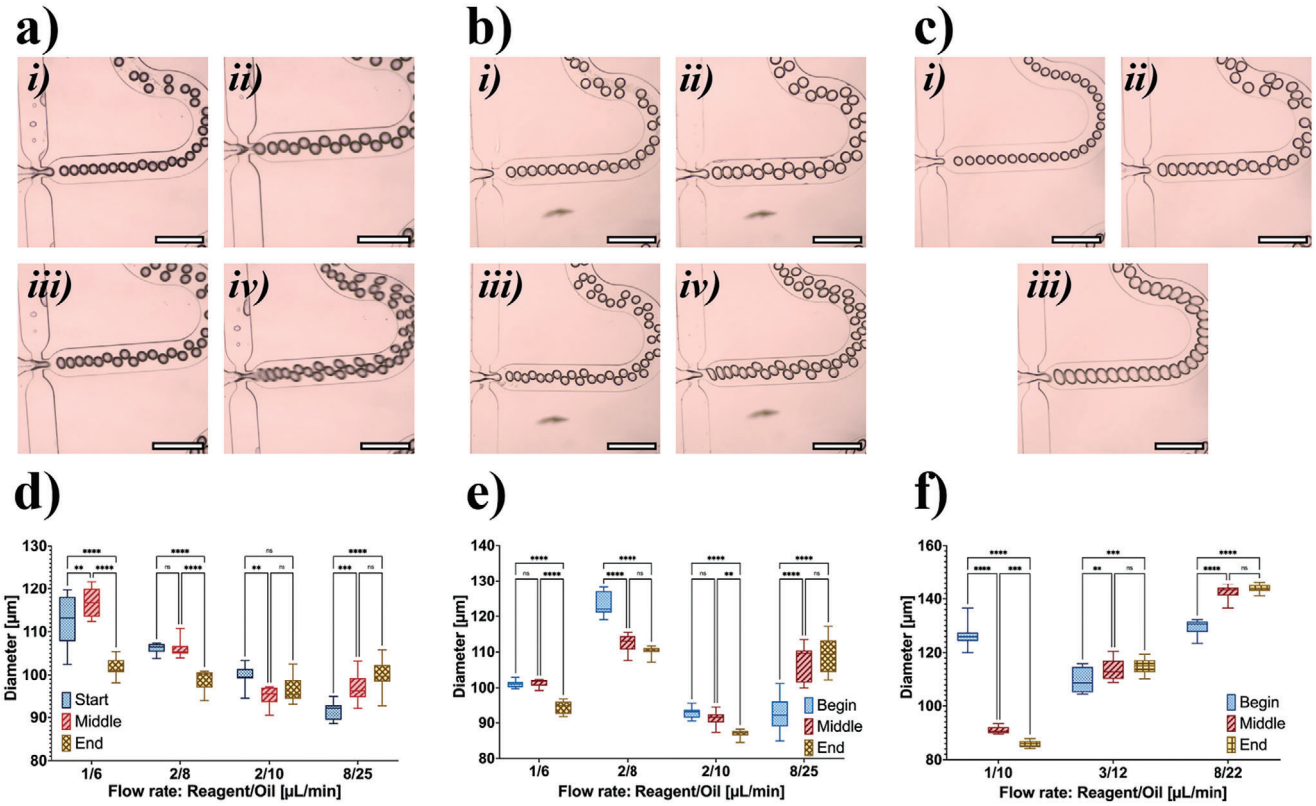

Figure 2. Droplets production stability test with a focus on surfactants, scale bar of 500 µm. a) Representative optical microscope images of droplet production in System A (CTAC-based mineral oil) with four flow rates (reagents/oil [µL min^{-1}]) of 1/6, 2/8, 2/10, 8/25 (from i to iv respectively), scale bar of 500 µm. b) Representative optical microscope images of droplet production in System B (CTAC-based mineral oil with depleted CATC in Octa-AuNPs solution) with four flow rates (reagents/oil [µL min^{-1}]) of 1/6, 2/8, 2/10, 8/25 (from i to iv respectively), scale bar of 500 µm. c) Representative optical microscope images of droplet production in System C (surfactant-free mineral oil) with four flow rates (reagents/oil [µL min^{-1}]) of 1/10, 3/12, 8/22 (from i to iii respectively), scale bar of 500 µm. d–f) Boxplots of the droplet sizes in the three systems at three time points (start, middle, and end of the reaction) with corresponding flowrates.

production. Subsequently, the proposed design was fabricated at 100 µm thickness. Figure 1e,f is exemplary pictures of droplet production using the fabricated device, showing good agreement with the simulation.

2.1.2. Droplet Stability Test

Droplet production is highly dependent on the effectiveness of the surfactant to reduce the surface energy.[54] Translating the bulk synthesis of gold nanoparticles (AuNPs) into the droplet microfluidics demand further understanding of additional effects from other foreign surfactants. Commonly, cetyltrimethylammonium chloride (CTAC) and cetyltrimethylammonium bromide (CTAB) are used in numerous protocols for AuNPs synthesis.[55–57] However, the use of foreign surfactant such as tween-20 to stabilize droplet formation in the microfluidic device may have their unpredictable effects on 1) the droplet stability when mixed with the stabilizing agents (CTAC and CTAB), and 2) on the morphological change of nanoparticles.[58–60] Hence, to simplify the reaction system, no foreign surfactants were used, and a screening test was evaluated in three systems (system A, B, and C). For all the systems, the reagents are CTAC stabilized octahedron gold nanoparticles (Octa-AuNPs) seed solution, and a growth solution (comprised of ascorbic acid, CTAB, L-glutathione, and $HAuCl_4$). Simply, the Octa-AuNPs solution is referred as the seed reagent solution. In system A, mineral oil with CTAC (5% w/v) was used as the continuous phase along with the two reagent solutions mentioned above. In system B, the seed solution was centrifuged to deplete the existing stabilizing agent CTAC, and the continuous phase was mineral oil with CTAC at 5% w/v while no amends were made to the growth solution. In system C, pure mineral oil was used without any addition of surfactants and there was no modification to seed solution and growth solution. One way to assess the droplet formation is to monitor the droplet size during the entire process of the collection, that is at the beginning of the collection, midway, and at the end time point, as shown in **Figure 2**a–c.

The objective is to identify optimal flow rates that achieve two main criteria: 1) maintaining a high speed with minimal impact on droplet size during collection, and 2) ensuring the camera can capture real-time imaging without deformation of droplets due to frame rate limitations. Variations in droplet size can influence particle synthesis by altering surface areas. The necessity for real-time monitoring of droplet formation to confirm consistent production dictates that the flow rate must be adjusted to accommodate the camera's limited capabilities. Too slow of a flow

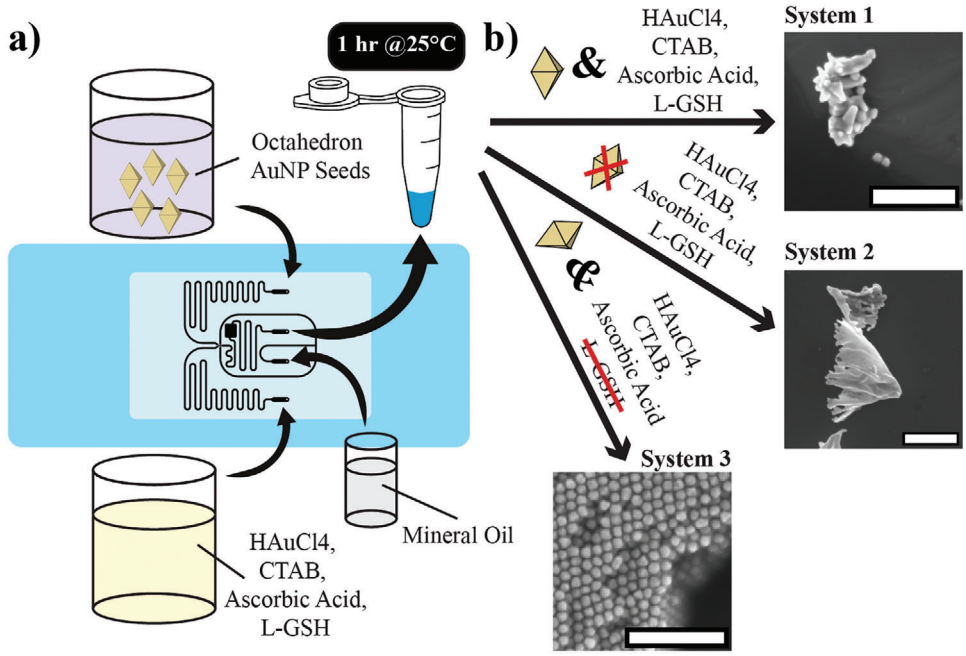

Figure 3. Schematic representation of the synthesis scheme and representative (nano-/micro-)particle morphologies, all scale bars of 500 nm. a) Two-reagent systems for the synthesis of gold (nano-/micro-)particles. The octahedron gold nanoparticles (Octa-AuNPs) and the growth solution, containing gold chloride solution ($HAuCl_4$), cetyltrimethylammonium bromide (CTAB), ascorbic acid (AA), and L-glutathione (L-GSH), are fed through the two inlets. Mineral oil, with/without cetyltrimethylammonium chloride (CTAC), is the continuous phase. The droplets are collected at in an Eppendorf tube and incubated for one hour at room temperature (approximately 25 °C). b) Schematic representation of the three systems with representative scanning electron images (SEM).

rate may result in prolonged collection of reaction fluid, where it may result in temporal variations, that is the first time point of droplets will have a substantially longer reaction time compared to the last time-point of droplets under the low flowrates. Thus, a sufficiently high flow rate without compromising real-time monitoring is desirable.

System A and system B differ at the concentration of CTAC, while the two systems' oil both contained CTAC at 5% w/v, the seed solution of system B had depleted CTAC by centrifuge. Interestingly, the average droplet size showed fluctuations for the chosen flow rates shown in Figure 2a,b. The droplet in system A and system B would have two surfactants (CTAC and CTAB) dynamically exchange at the interface to achieve stability and ensures that the aqueous phase remains segmented in the continuous oil phase.[56,61,62] The change in flow rate would change the amount of CTAC/CTAB availability at the interface; thus, showing an unpredictable trend. However, in system C where no surfactant is added to mineral oil. The increase of flow rates, especially the continuous phase, would have minimal impact on the availability of CTAC in the droplets. Hence, the dynamic change of the droplet sizes in system C is much more linear. We chose a final flow rate of 8/22 [μL min^{-1}] for the reagent/oil from system C for the particle synthesis thanks to the relatively good stability and a sufficiently fast rate.

2.2. Synthesis of Gold Nano-/Microparticles

The synthesis scheme of the anisotropic particles is depicted in **Figure 3**. The octahedron gold nanoparticles (Octa-AuNPs) were synthesized according to previously reported method prior to its use in microfluidic-assisted synthesis.[63,64] The average diameter of Octa-AuNPs, measured by its major axis, is determined to be 27.46 ± 0.39 nm and with a peak absorbance at 565 nm (Figure S7b, Supporting Information). For the two-reagent microfluidics, the Octa-AuNPs solution is fed through one of the inlets without mixing any other chemicals; while the other inlet is fed with growth solution, containing gold ions, CTAB, ascorbic acid, and L-glutathione (L-GSH), as depicted in Figure 3a. For the production of particles, we followed system C: flow rates of reagents/oil:8/22 [μL min^{-1}] with pure mineral oil.

We adapted all the chemicals of Lee et al. work to the droplet microfluidic system,[23] and the scanning electron microscopy (SEM) images showed surprising anisotropic particles at micron sizes. An energy-dispersive X-ray analysis (EDXA) was performed on the samples and confirmed gold element composition (Figure 5). To decouple the reaction scheme, two other reaction schemes were investigated, as indicated in Figure 3b. Results from system 1 showed anisotropic structures similar to previously reported structures.[65,66] However, the branches showed significant elongation (**Figure 4**). Further, it is possible to observe that satellite AuNPs are present in the background or adhering the micro-particle.

The origin of the smaller nanoparticles was unknown but suspected to be of L-GSH induced synthesis of AuNPs. To examine this theory indirectly, two other systems were investigated. Concerning the seed solution may act as growth site for the reduced Au^{1+} ions, System 2 excluded the use of Octa-AuNPs and System 3 excluded the use of L-GSH. Surprisingly, as shown in Figure 3b, even in the absence of Octa-AuNPs (the seed), large

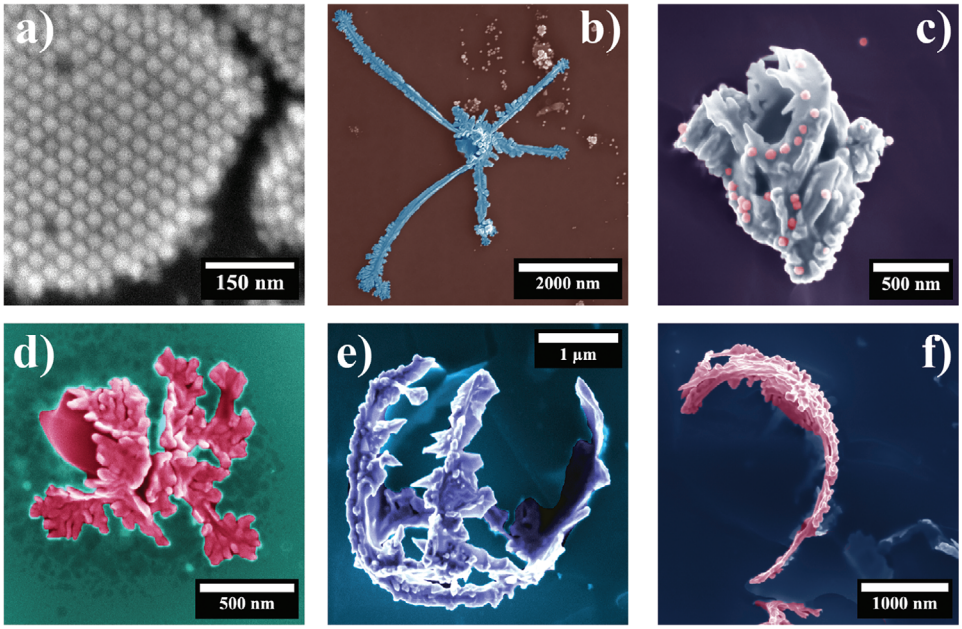

Figure 4. Representative scanning electron images (SEM) from System 1. a) SEM image of octahedron gold nanoparticles (Octa-AuNPs) with an average diameter of 27.46 ± 0.39 nm (Supporting Information). b–f) Representative SEM images of the droplet-assisted production of branched (nano-/micro-)particles from b–d) system 1 and e,f) 2, scale bars as shown.

particles were produced, suggesting a potential seedless synthesis of gold nanoparticles mediated by L-GSH. Since there were no seed particles present in the reagents, the formation of fan-shaped particles could only be a direct result from the reduction of Au^{1+} to Au^{0} by L-GSH.[67] While the observed large fan-shaped particles are of surprise, the presence of smaller satellite particles in the background is consistent with literature reports (Figures S1 and S2, Supporting Information), similar to previous reported seedless synthesized AuNPs.[68]

Several hyper-branched structure and elongated structure were found in the products of System 1 and System 2 (Figure 4b–f). It is evident that despite overall enlarged morphology, the gold microparticles (AuMPs) still retains fine features of sub 100 nm dendritic branches. In some cases, spherical nanoparticles showed attachment to the large AuMPs as shown in Figure 4c. To confirm that the particles are indeed of element gold, SEM-EDXA was conducted. Encouragingly, all the branched structures exhibited positive screening of element

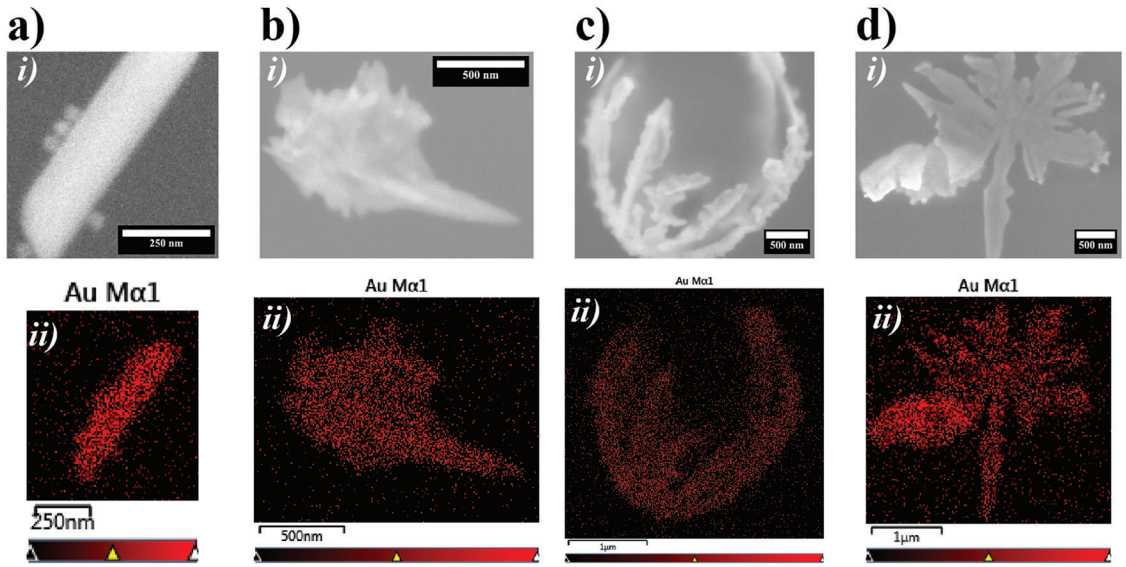

Figure 5. Scanning electron images (SEM, top images) and energy dispersive X-ray (EDS, bottom images) of selected nano-/micro-particles. a) A gold nano-bar, scale bar of 250 nm. b) A gold nano-spike, scale bar of 500 nm. c) A gold microcrown, scale bar of 500 nm (SEM) and 1 µm (EDS). d) A gold-maple leaf, scale bar of 500 nm (SEM) and 1 µm (EDS).

gold, shown in **Figure 5**. Thus, to the best of our knowledge, this work would be the first account of the synthesis of microscale anisotropic gold particles using droplet microfluidics.

In contrast, results from System 3 where the absence of L-GSH showed dormant growth of Octa-AuNPs where visible truncated structures were observed on the surface, implying a likely consequence of the further growth of Octa-AuNPs.[69] To summarize, these results suggested that L-GSH not only had the ability to direct further gold nanoparticle growth, but it also demonstrated its ability to reduce Au^{1+} to Au^{0} and facilitate hyper growth at the water/oil interface.

While we cannot fully explain the exact mechanisms behind the formation of gold microparticles, we suspect that interactions at the oil/water interface play a critical role in this observation. Previously, Shin et al. demonstrated that inducing an emulsion system could produce branched AuNPs, although these anisotropic AuNPs were significantly smaller than the sizes we observed.[46] Lee et al.'s studies showed that microdroplets at the air/water interface could produce AuNPs with a kinetic profile showing a fivefold increase, observing spontaneous AuNP formation without a reducing agent or externally applied charge.[70] Thus, an accelerated kinetic reaction at the oil/water interface might also hold true for our systems, leading to the spontaneous formation of satellite AuNPs. The inclusion of system 3 further underscores the role of L-GSH in not only reducing Au [I+] into gold atoms but also in facilitating the formation of elongated branches.[47,71] L-GSH might self-assemble into oligomers or aggregate Au [I] complexes, suggesting that nanoparticles could self-assemble at the oil/water interface to act as a template,[72–74] with interactions with L-GSH further assisting in the reduction of Au [I+] into gold atoms at the self-assembled layer.[67,71] While current synthesis methods produce random structures, a more controlled morphology could be achieved by better understanding these reaction schemes, specifically by leveraging the combined effects of accelerated droplet interfacial kinetics and L-GSH's directed synthesis capability.

3. Conclusion

In conclusion, we have demonstrated the synthesis of gold microparticles (AuMPs) via peptide-directed seed-mediated methods in conjunction with droplet microfluidics. Small gold nanoparticles are formed in the presence of a tripeptide, L-GSH (L-glutathione), without the need of a strong reducing agent. Further, the inclusion of L-GSH has been demonstrated to play a crucial role in facilitating anisotropic morphologies. The droplets provide a necessary reaction condition for the dendritic particles at the oil/water interface. The synthesis method described herein is an attempt to translate the peptide directed nanoparticle synthesis method to a droplet microfluidic platform, demonstrating the advantages of not requiring long reaction times, temperatures, or templates to produce the asymmetric gold particles. From a synthesis standpoint, the droplet microfluidic platform can be a perfect tool for the study of interfacial synthesis of gold nanoparticles. While the potential applications of these synthesized anisotropic gold nano-/microparticles were not explored, it is reasonable to predict that these structures may have a substantial impact on catalysis, biosensing, and other field of research due to the unusual high surface area. Further, the optical properties of these structures may need to be looked upon for to understand whether they possess chiroptical or near-/far-field optical properties.

4. Experimental Section

Experimental section is given in the Supporting Information.

Supporting Information

Supporting Information is available from the Wiley Online Library or from the author.

Acknowledgements

The authors acknowledge the facilities as well as the scientific and technical assistance of the Research and Prototype Foundry Core Research Facility at the University of Sydney, part of the NSW node of the NCRIS-enabled Australian National Fabrication Facility. The authors thank the volunteers, Ms. Yasyika Alegesam and Ms. Clarissa Ayoub, for their contribution to the project. Ms. Yasyika Alegesam helped with the synthesis of octahedron gold nanoparticle in the early stage of the project. Ms. Clarissa Ayoub helped with the microfluidic setup. This work was supported by the University of Sydney Nano Institute HDR Development Award (HDA) to Mr. Zhenxu Yang. This work was partially supported by the Australia-India Strategic Research Fund (AISRF).

Open access publishing facilitated by The University of Sydney, as part of the Wiley - The University of Sydney agreement via the Council of Australian University Librarians.

Conflict of Interest

The authors declare no conflict of interest.

Data Availability Statement

The data that support the findings of this study are available from the corresponding author upon reasonable request.

Keywords

dendritic particles, droplet microfluidics, emulsion, gold nanoparticle, simulation

Received: March 25, 2024
Revised: May 13, 2024
Published online: June 7, 2024

[1] F. Tian, L. Cai, C. Liu, J. Sun, *Lab Chip* **2022**, *22*, 512.
[2] S. Abalde-Cela, P. Taladriz-Blanco, M. G. De Oliveira, C. Abell, *Sci. Rep.* **2018**, *8*, 2440.
[3] X. Chen, H. Lv, *NPG Asia Mater.* **2022**, *14*, 69.
[4] H. Tao, T. Wu, S. Kheiri, M. Aldeghi, A. Aspuru-Guzik, E. Kumacheva, *Adv. Funct. Mater.* **2021**, *31*, 2106725.
[5] J. Kotouček, F. Hubatka, J. Mašek, P. Kulich, K. Velínská, J. Bezděková, M. Fojtíková, E. Bartheldyová, A. Tomečková, J. Stráská, D. Hrebík, S. Macaulay, I. Kratochvílová, M. Raška, J. Turánek, *Sci. Rep.* **2020**, *10*, 5595.

[6] M. Omidi, M. Hashemi, L. Tayebi, *RSC Adv.* **2019**, *9*, 33246.
[7] G.-X. Li, Q. Li, R. Cheng, S. Chen, *Curr. Opin. Chem. Eng.* **2020**, *29*, 34.
[8] P. Stolzenburg, T. Lorenz, A. Dietzel, G. Garnweitner, *Chem. Eng. Sci.* **2018**, *191*, 500.
[9] J. Wang, Y. Song, *Small* **2017**, *13*, 1604084.
[10] S. Gimondi, H. Ferreira, R. L. Reis, N. M. Neves, *ACS Nano* **2023**, *17*, 14205.
[11] O. Marom, F. Nakhoul, U. Tisch, A. Shiban, Z. Abassi, H. Haick, *Nanomedicine* **2012**, *7*, 639.
[12] J. Sun, Y. Xianyu, X. Jiang, *Chem. Soc. Rev.* **2014**, *43*, 6239.
[13] M. Hegde, P. Pai, M. G. Shetty, K. S. Babitha, *Environ. Nanotechnol., Monit. Manage.* **2022**, *18*, 100756.
[14] H. Chen, X. Zhang, S. Dai, Y. Ma, S. Cui, S. Achilefu, Y. Gu, *Theranostics* **2013**, *3*, 633.
[15] M. Ma, H. Chen, Y. Chen, X. Wang, F. Chen, X. Cui, J. Shi, *Biomaterials* **2012**, *33*, 989.
[16] H. Daraee, A. Eatemadi, E. Abbasi, S. Fekri Aval, M. Kouhi, A. Akbarzadeh, *Artif. Cells Nanomed. Biotechnol.* **2016**, *44*, 410.
[17] A. H. Ahamed Fazil, U. S. Reddy, M. Bhargavi Gumpu, in *Health and Environmental Applications of Biosensing Technologies*, Elsevier, Amsterdam **2024**, pp. 267–291.
[18] N. C. Dalibera, M. J. Rodrigues-Jesus, R. Andreata-Santos, L. M. Ramos Janini, A. F. Oliveira, A. Rodrigues Azzoni, L. C. De Souza Ferreira, M. T. P. Favaro, *ACS Appl. Nano Mater.* **2023**, *6*, 22774.
[19] N. Milivojević, M. R. Carvalho, D. Caballero, S. Radisavljević, M. Radoićić, M. Živanović, S. C. Kundu, R. L. Reis, N. Filipović, J. M. Oliveira, *Nanomedicine* **2024**, *19*, 483.
[20] K. Curtin, T. Godary, P. Li, *Microfluid. Nanofluid.* **2023**, *27*, 77.
[21] X. Zhang, S. Ma, A. Li, L. Chen, J. Lu, X. Geng, M. Xie, X. Liang, Y. Wan, P. Yang, *Appl. Nanosci.* **2020**, *10*, 661.
[22] Y. Hang, A. Wang, N. Wu, *Chem. Soc. Rev.* **2024**, https://doi.org/10.1039/D3CS00793F.
[23] H.-E. Lee, H.-Y. Ahn, J. Mun, Y. Y. Lee, M. Kim, N. H. Cho, K. Chang, W. S. Kim, J. Rho, K. T. Nam, *Nature* **2018**, *556*, 360.
[24] H. Kim, S. W. Im, N. H. Cho, D. H. Seo, R. M. Kim, Y. Lim, H. Lee, H. Ahn, K. T. Nam, *Angew. Chem.* **2020**, *132*, 13076.
[25] C. Zhang, Z. Zhou, X. Zhi, Y. Ma, K. Wang, Y. Wang, Y. Zhang, H. Fu, W. Jin, F. Pan, D. Cui, *Theranostics* **2015**, *5*, 134.
[26] Z. Hu, D. Meng, F. Lin, X. Zhu, Z. Fang, X. Wu, *Adv. Opt. Mater.* **2019**, *7*, 1801590.
[27] Z. Yang, A. Jaiswal, Q. Yin, X. Lin, L. Liu, J. Li, X. Liu, Z. Xu, J. J. Li, K.-T. Yong, *Nanoscale* **2024**, *16*, 5014.
[28] N. Cherkasov, Y. Bai, A. J. Expósito, E. V. Rebrov, *React. Chem. Eng.* **2018**, *3*, 769.
[29] O. Długosz, M. Banach, *React. Chem. Eng.* **2020**, *5*, 1619.
[30] F. Ejeta, *Drug Des., Dev. Ther.* **2021**, *15*, 3881.
[31] S. K. Bhargava, J. M. Booth, S. Agrawal, P. Coloe, G. Kar, *Langmuir* **2005**, *21*, 5949.
[32] T. Maruyama, Y. Fujimoto, T. Maekawa, *J. Colloid Interface Sci.* **2015**, *447*, 254.
[33] Y. Li, Z. Tang, P. N. Prasad, M. R. Knecht, M. T. Swihart, *Nanoscale* **2014**, *6*, 3165.
[34] Y. N. Tan, J. Y. Lee, D. I. C. Wang, *J. Am. Chem. Soc.* **2010**, *132*, 5677.
[35] H.-C. Chu, C.-H. Kuo, M. H. Huang, *Inorg. Chem.* **2006**, *45*, 808.
[36] T. Huang, F. Meng, L. Qi, *Langmuir* **2010**, *26*, 7582.
[37] J. Kim, Y. Rheem, B. Yoo, Y. Chong, K. N. Bozhilov, D. Kim, M. J. Sadowsky, H.-G. Hur, N. V. Myung, *Acta Biomater.* **2010**, *6*, 2681.
[38] N. Li, P. Zhao, D. Astruc, *Angew. Chem., Int. Ed.* **2014**, *53*, 1756.
[39] N. Y. Hau, P. Yang, C. Liu, J. Wang, P.-H. Lee, S.-P. Feng, *Sci. Rep.* **2017**, *7*, 39839.
[40] D. J. Magdalene, D. Muthuselvam, T. Pravinraj, *Appl. Nanosci.* **2021**, *11*, 2073.
[41] M. B. Kulkarni, S. Goel, *Nano Express* **2020**, *1*, 032004.
[42] K. Sugano, Y. Uchida, O. Ichihashi, H. Yamada, T. Tsuchiya, O. Tabata, *Microfluid. Nanofluid.* **2010**, *9*, 1165.
[43] G. A. Vinnacombe-Willson, J. K. Lee, N. Chiang, L. Scarabelli, S. Yue, R. Foley, I. Frost, P. S. Weiss, S. J. Jonas, *ACS Appl. Nano Mater.* **2023**, *6*, 6454.
[44] A. Agha, W. Waheed, I. Stiharu, V. Nerguizian, G. Destgeer, E. Abu-Nada, A. Alazzam, *Discovery Nano* **2023**, *18*, 18.
[45] V. Sebastian Cabeza, S. Kuhn, A. A. Kulkarni, K. F. Jensen, *Langmuir* **2012**, *28*, 7007.
[46] Y. Shin, C. Lee, M.-S. Yang, S. Jeong, D. Kim, T. Kang, *Sci. Rep.* **2014**, *4*, 6119.
[47] N.-N. Zhang, H.-R. Sun, Y. Xue, F. Peng, K. Liu, *J. Phys. Chem. C* **2021**, *125*, 10708.
[48] S. Duraiswamy, S. A. Khan, *Part. Part. Syst. Charact.* **2014**, *31*, 429.
[49] L. Uson, V. Sebastian, M. Arruebo, J. Santamaria, *Chem. Eng. J.* **2016**, *285*, 286.
[50] T. M. Ho, A. Razzaghi, A. Ramachandran, K. S. Mikkonen, *Adv. Colloid Interface Sci.* **2022**, *299*, 102541.
[51] S. Sachdev, R. Maugi, J. Woolley, C. Kirk, Z. Zhou, S. D. R. Christie, M. Platt, *Langmuir* **2017**, *33*, 5464.
[52] L. M. Caballero-Aguilar, S. Duchi, A. Quigley, C. Onofrillo, C. Di Bella, S. E. Moulton, *MethodsX* **2021**, *8*, 101324.
[53] S. D. Shingte, O. Altenburg, P. J. T. Verheijen, H. J. M. Kramer, H. B. Eral, *Cryst. Growth Des.* **2022**, *22*, 4072.
[54] E. Zdrali, G. Etienne, N. Smolentsev, E. Amstad, S. Roke, *J. Chem. Phys.* **2019**, *150*, 204704.
[55] Y. Inoue, Y. Tsutamoto, D. Muko, K. Nanamura, T. Sawada, Y. Niidome, *Anal. Sci.* **2016**, *32*, 875.
[56] Y. Song, M. Zhang, H. Fang, H. Xia, *ChemPhysMater* **2023**, *2*, 97.
[57] S. K. Meena, S. Celiksoy, P. Schäfer, A. Henkel, C. Sönnichsen, M. Sulpizi, *Phys. Chem. Chem. Phys.* **2016**, *18*, 13246.
[58] N. Wu, Y. Zhu, P. W. Leech, B. A. Sexton, S. Brown, C. Easton, in (Eds: D. V. Nicolau, D. Abbott, K. Kalantar-Zadeh, T. Di Matteo, S. M. Bezrukov), Canberra, ACT, Australia **2007**, p. 67990C.
[59] J. H. Xu, P. F. Dong, H. Zhao, C. P. Tostado, G. S. Luo, *Langmuir* **2012**, *28*, 9250.
[60] N. M. Kovalchuk, M. J. H. Simmons, *Adv. Colloid Interface Sci.* **2023**, *312*, 102844.
[61] E. B. Abuin, M. A. Rubio, E. A. Lissi, *J. Colloid Interface Sci.* **1993**, *158*, 129.
[62] P. Basuri, A. Chakraborty, T. Ahuja, B. Mondal, J. S. Kumar, T. Pradeep, *Chem. Sci.* **2022**, *13*, 13321.
[63] P. Chung, L. Lyu, M. H. Huang, *Chem. - Eur. J.* **2011**, *17*, 9746.
[64] G. Singh, H. Jami, P. Lesani, S. Bhattacharya, Y. Ramaswamy, P. B. Bisht, H. Zreiqat, *Nano Res.* **2022**, *15*, 1260.
[65] Y. Li, M. Zhai, H. Xu, *Appl. Surf. Sci.* **2019**, *498*, 143864.
[66] V. S. Gummaluri, R. Gayathri, C. Vijayan, V. M. Murukeshan, *J. Opt.* **2020**, *22*, 065003.
[67] X. Mao, Z.-P. Li, Z.-Y. Tang, *Front. Mater. Sci.* **2011**, *5*, 322.
[68] P. Choo, D. Arenas-Esteban, I. Jung, W. J. Chang, E. A. Weiss, S. Bals, T. W. Odom, *ACS Nano* **2022**, *16*, 4408.
[69] M. Kim, H.-J. Park, P. 한상우, Y. Jimin, W.-S. Yun, *Bull. Korean Chem. Soc.* **2013**, *34*, 2243.
[70] J. K. Lee, D. Samanta, H. G. Nam, R. N. Zare, *Nat. Commun.* **2018**, *9*, 1562.
[71] W. Wang, Y. Han, J. Zhu, Y. Fan, Y. Wang, *J. Nanopart. Res.* **2019**, *21*, 24.
[72] D. Wang, H. Duan, H. Möhwald, *Soft Matter* **2005**, *1*, 412.
[73] G. Yang, D. T. Hallinan, *Sci. Rep.* **2016**, *6*, 35339.
[74] T. Ding, A. W. Rudrum, L. O. Herrmann, V. Turek, J. J. Baumberg, *Nanoscale* **2016**, *8*, 15864.

